Latest HOT II-VI technologies development at LYNRED

L. Rubaldo[(1)], C. Grezes, [(1)],N. Morisset[(1)], ,C. Cassillo[(1)], J. Berthoz[(1)], A. Brunner[(1)], O. Gravrand[(2)], C. Lobre[(2)], N. Baier[(2)], P. Jenouvrier[(1)]

[(1)] *LYNRED, Technologies and Products Department, ZI, BP21, 38113 Veurey-Voroize. FRANCE*
laurent.rubaldo@lynred.com
[(2)] *CEA Leti – MINATEC, 17 rue des Martyrs, 38054 Grenoble Cedex 9, France*

KEYWORDS: II-VI, MW, LW, VLW, HOT, SXGA, QE, 7.5µm pitch, MTF, RFPN, Temporal Noise, RTS.

ABSTRACT

LYNRED is a leading global supplier of high-quality II-VI and III-V infrared detectors, as well as bolometers, to the aerospace, defence, and commercial markets. Our vision is to preserve and protect, providing the right technology to meet our customers' needs. In order to consolidate our position as a leading manufacturer of infrared detectors and respond to growing market demand for next-generation infrared technologies, we are breaking ground on a new state-of-the-art industrial facility. Named Campus, this new industrial site will double the current cleanroom footprint and increase production capacity, offering an optimal cleanliness classification for new high-performance products.

Campus will support the ongoing development, particularly of sub-10 µm pitch cooled infrared detectors, including MCT for extended MW band applications, as well as LW and VLW technologies.

We will review the latest developments on II-VI HOT FPA (Focal Plane Array) and IDDCA (Integrated Detector Dewar Cryocooler Assembly) with 7.5µm pitch focal plane array in SXGA format with a digital ROIC to cover extended MW band applications and customer needs in a comprehensive and versatile way. We will highlight the latest results in terms of low frequency noise, stability and reproducibility of Residual Fixed Pattern Noise (RFPN) up to 150K and Modulation Transfer Function (MTF) optimisations. We will also present our recent QXGA format developments. Finally, recent results on the development of LW and VLW focal plane arrays with cut-off wavelength up to 15µm will be addressed.

1. INTRODUCTION

To address the challenge posed by low SWaP-C (size, weight, and power cost), LYNRED is developing High Operating Temperature (HOT) II-VI technology to meet the requirements of demanding applications. Significant advancements have been made in the field of HOT technology. With regard to the extended MW band and p-on-n technology, remarkably high EQE of almost 85% and MTF of over 0.5 at Nyquist frequency have been achieved. These achievements are complemented by the demonstration of low, stable spatio-temporal noise up to 150 K. The ongoing development of the VLW band and LW optimisations is showing promising results. The VLW band has very high operability up to 80 K, with a cut-off wavelength of 15 µm.

The section 2 of this paper will be dedicated to latest results on extended MW IDDCAs with SXGA format and 7.5µm pitch, in terms of MTF, RFPN, image quality and noise study. The section 3 will show the recent results on QSXGA format development based on the same technology and pitch. In section 4 we will focus on LW p-on-n technology optimization. Before concluding in section 6, the section 5 will show some remarkable results on on-going VLW development addressing cut-off wavelength up to 15µm at 80K.

2. SXGA 7.5µm PITCH FPA PERFORMANCES EXTENDED MW BAND

2.1. ROIC KEY FEATURES

A new digital ROIC in SXGA format (1280x1024) with 7.5 µm pitch has been designed in-house and manufactured by an advanced silicon CMOS foundry for both III-V and II-VI technologies. The table below summarises the main features. Very good linearity has been achieved for this 14-bit digital ROIC, less than 0.5%, with an appropriate power consumption of 100mW at full frame rate.

	7.5µm pixel pitch ROIC
Format	1280x1024 (SXGA)
Integration modes	Snapshot - ITR/IWR
Storable charges	0.41Me-, 0.7Me-, 1.1Me-
Linearity	+/- 0.5%
Consumption	100mW (full frame)
Frame Rate	60Hz (full format)
Functions	Windowing, Line/row inversion, Image rotation, 2x2 bining…

Table 1 : SXGA 7.5µm pitch Read Out Integrated Circuit characteristics.

2.2. QUANTUM EFFICIENCY

To address the full MW band, MCT p-on-n technology [1], is used with the latest improvements. Thanks to the dark current limited by the Auger 1 recombination mechanism [2], this technology meets the HOT requirements with an operating temperature of 130K. The graph below shows the normalised external quantum efficiency as a function of wavelength. .

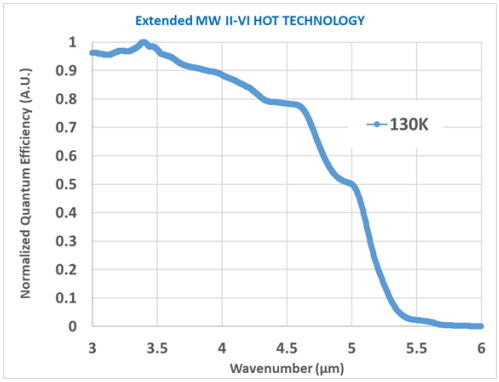

Figure 1: Normalized quantum efficiency at 130K –p-on-n technology 7.5µm pitch

A cut-off wavelength of 5µm at 130K is achieved, and compared to previous performance an improvement of 10 points has been achieved by optimising the collection volume, with an average External Quantum Efficiency (EQE) in the [3.7µm, 4.8µm] range of around 85%±5.

2.3. OPERABILITY

A state-of-the-art flip chip with indium bumps has been realized on in-house post-processed ROIC wafers to ensure perfect operability at production level combined by the absence of excess noise as illustrated by the noise operability distribution function shown below, with a median value above 99.95%, with a criteria mean RMS noise ± 100%.

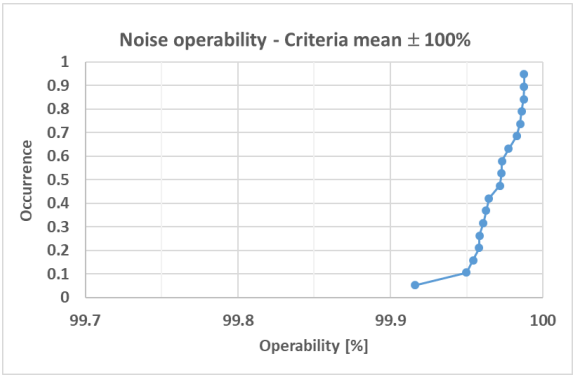

Figure 2 : Noise operability distribution function – 130K F/3 – SXGA 7.5µm pitch

2.4. MTF

The MTF performance is a key performance to ensure, on the one hand, a high image quality and, on the other hand, a high range, provided that a high quantum efficiency and a low temporal and spatial noise are maintained.
MTF is measured with a knife edge method [3]. This technique has been used successfully in the past from 30µm to 10µm [4] pixel pitch. The measured MTF is not directly the pixel MTF due to the optical bench contribution. Aberration and diffraction have to be taken into account to extract accurately the pixel MTF [4].

$$MTF_{measured} = MTF_{pixel} \times MTF_{optical} \qquad \text{Eq.1}$$

By playing with the diode design to optimize the collection and diffusion volumes, and taking advantage of the isotropic transport in the bulk CdHgTe alloy, planar structure could be kept and a high MTF could be obtained. This is illustrated below, where the first design (V1) is compared to the last optimized one (V3). An MTF improvement of 6 points is achieved at nominal diode polarisation while maintaining a high quantum efficiency of 85%±5%, and a remarkable value of 0.52±0.02 is obtained at Nyquist frequency (66mm^{-1}).

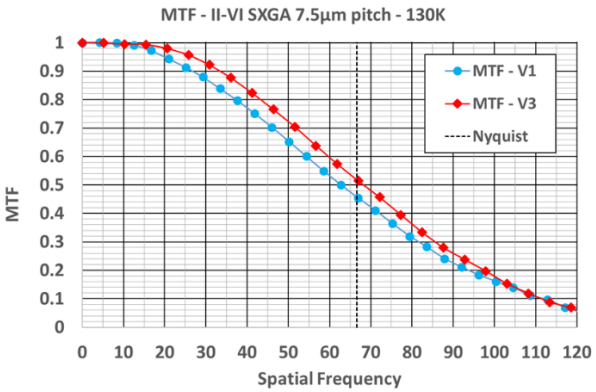

Figure 3 : MTF improvement – 130K – 7.5µm pitch p-on-n technology

2.5. RFPN PERFORMANCE

RFPN is defined as the standard deviation of the output signal over all pixels of the FPA, after Non-Uniformity Correction (NUC). It is a key performance indicator of image quality. In addition, RFPN degradation could reduce the system range, which is detrimental to IRST systems. For different process versions, the RFPN performance during the first cool down is illustrated in the graph below, where the RFPN to RMS noise ratio is plotted against well fill. We can see comparable and remarkable performances for the three versions of the II-VI technology. An RFPN/RMS noise ratio well below unity is achieved in the well fill range [10%, 85%], event below 0.5 in the range [15%, 85%].

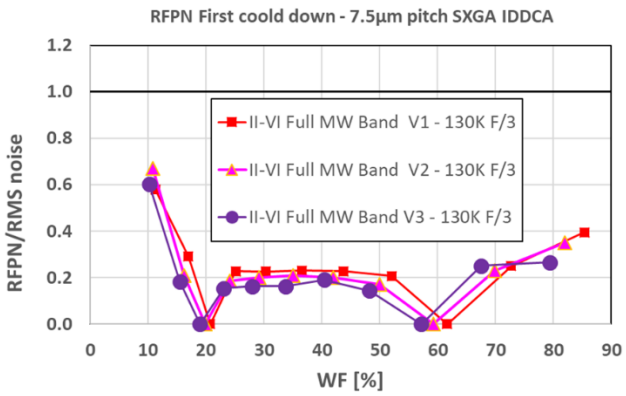

Figure 4 : RFPN to RMS noise ratio at 130K - SXGA products format 7.5µm pitch IDDCA F/3 aperture

RFPN Reproducibility is improved between V1 and V2. Using factory NUC table, RFPN is measured over several days with only one point refreshment (acting like offset correction). The RFPN/RMS noise ratio is illustrated below and shows a reduction of almost 20%, with a ratio value of less than one for the V2 design over the entire well fill range [15%, 85%].

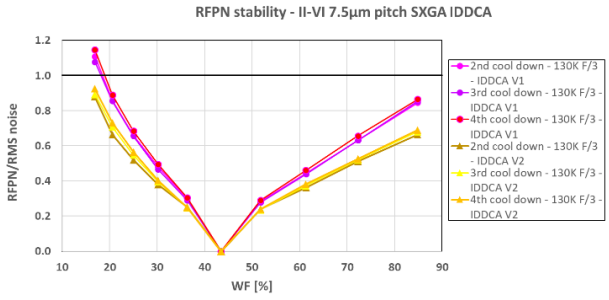

Figure 5: Stability of RFPN to RMS noise ratio after one point refreshment for both versions (V1 &V2) of SXGA format 7.5µm pitch IDDCA – F/3 aperture 130K

The latest optimized version, V3, offers the same RFPN stability over cool downs at 130K, but also an equivalent remarkable stability at 150K, as highlighted in the graph below where the RFPN/RMS ratio remains well below 0.5 for the first cool down, and below 0.8 for several cool downs over several days with only one point refreshment.

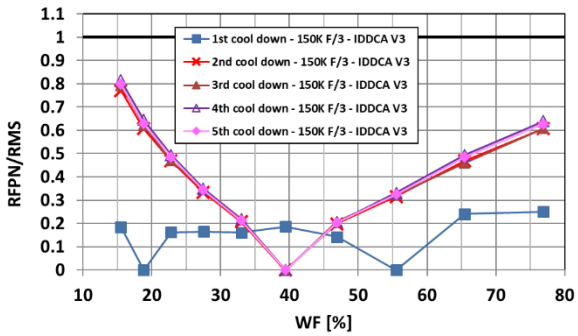

Figure 2 : Stability of RFPN to RMS noise ratio after one point refreshment for the latest V3 version - SXGA format 7.5µm pitch IDDCA – F/3 aperture 150K

This high correctability is complemented by a high image operability which includes classical criteria ((DC level ± 30%, Responsivity ± 20%, RMS noise ± 100%), and also includes RFPN defects defined by the expression below:

$$|NC_{corrected}(x,y) - \overline{NC_{corrected}}| > \overline{NC_{corrected}} \times \alpha \quad \text{Eq.2}$$

$$with\ \alpha \in [0.3\%, 0.5\%]$$

where $NC_{corrected}(x,y)$ is the 2-points corrected output level for diode (x,y) and $\overline{NC_{corrected}}$ the mean output corrected level of the FPA for a given black body temperature.

For this V3 version an image operability above 99.9% at 130K and above 99.7% at 150K, operability cumulated over 5 cool downs and 10 different black body temperatures for each cool down. This is summarized in the following table.

	Image operability cumulated over 5 cool downs, 10 black body temperatures for each cool down
130K	> 99.9%
150K	> 99.7%

Table 2: Image operability – SXGA format

2.6. LOW FREQUENCY NOISE AND RTN ISSUES

RTN or RTS (Random Telegraphic Signal) [5] pixels are a key issue in image calibration and correction. But more generally the low frequency noise defects (1/fn with n≥1) affect operability and image quality.

To demonstrate this for II-VI p-on-n HOT technology, we plot below for defective and non-defective pixels, the distribution function of normalized noise power spectral density (NPSD) for two different frequencies, 10Hz and 52 mHz. The NPSDs are normalised by the median value at 10 Hz for non-defective pixels.

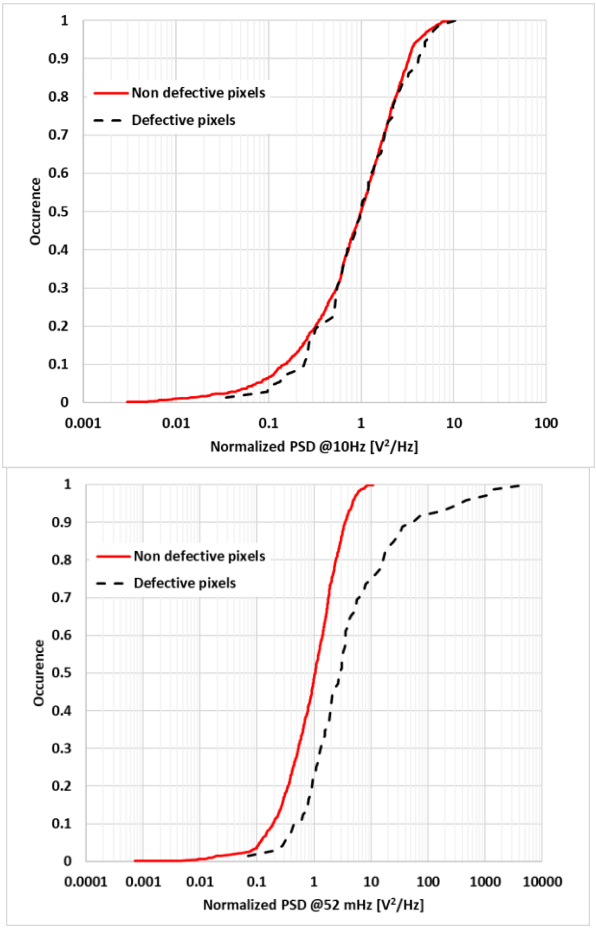

Figure 3 Distribution functions for Normalised Noise Power Spectral Density (NPSD) for defective and non-defective pixels at 10 Hz (right) and 52mHz (left) – SXGA Format 7.5µm II-VI technology – 130K F/3 aperture

It can clearly be seen that defective pixels have excess low frequency noise, with two distinct distribution functions at 52 mHz with a median value 3 times higher and distribution tail with a value two decades higher for defective pixels.

In order to investigate the provenance of such low frequency noise excess, spectroscopic studies of electrically active defects have been conducted utilizing the so-called Deep Level Transient Spectroscopy (DLTS) technique [6], [7]. This technique has already been successfully applied form SWIR to LWIR II-VI technologies [8],[9].

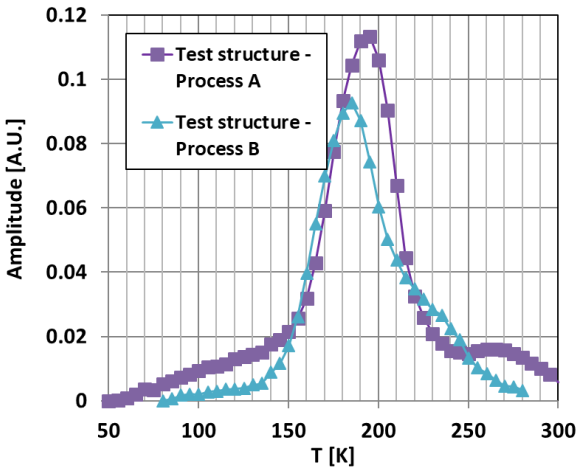

Figure 4 : DLTS scan for two different process versions - test structure

As shown for Process B, a DLTS peak with a lower amplitude is presented. It is important to note that peak amplitude is directly proportional to defect concentration. Research is underway to determine defects fingerprints like activation energy, capture cross section and nature of electrically defects. This investigative approach has yielded improvements in RTS defects. The graph below presents for II-VI SXGA FPA the RTS defects stability over time during the same cool-down for two distinct design versions. The measurements were taken over a period of one hour, with a detection criterion of three times RMS noise.

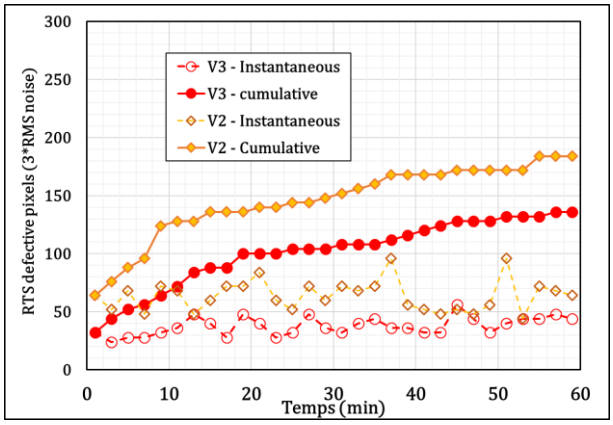

Figure 5 : RTS reproducibility for V2 and V3 design versions over 1h during same cool-down - FPA 7.5µm pitch SXGA format – 130K F/3

25% less RTS defects have been obtained for V3 design. At that time, the causal relationship between DLTS defects and RTS had not been established. However, a clear correlation between the concentration of electrically active defects and low-frequency noise defects has been demonstrated.

As a result, we have achieved an impressive reduction in RTS pixels, as demonstrated in the graph below for II-VI SXGA FPA with 7.5 µm pitch. The measurements were made over several cool-

downs, with 10000 frames acquired in total over 250 seconds. The detection criterion was set at three times the average root mean square (RMS) noise.

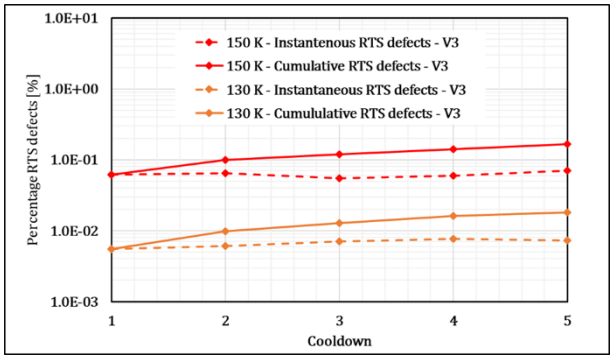

Figure 6 : RTS reproducibility for V3 design version over several cool-downs - FPA 7.5µm pitch SXGA format – 130K & 150K F/3

Cumulated over 5 cool-downs, less than 0.02% RTS defects have been obtained at 130K and less than 0.2% at 150K, F/3 aperture. The following section will present the latest results on QXGA FPA 7.5µm pitch using II-VI p-on-n technology.

3. QXGA 7.5µm PITCH EXTENDED MW PRODUCT DEVELOPMENT

3.1. ROIC DEVELOPMENT

For the future QXGA product, based on the SXGA ROIC development, a new digital ROIC has been designed in-house and manufactured by an advanced silicon CMOS foundry. The table below summarises the main features. Very good linearity has again been achieved for this 14-bit digital ROIC, less than 0.5%, with a frame rate of up to 100 Hz.

	7.5µm pixel pitch ROIC
Format	1920x1536 (QXGA)
Integration modes	Snapshot - ITR/IWR
Storable charges	0.35Me-, 0.9Me-, 1.44Me-
Linearity	+/- 0.5%
Consumption	400mW (full frame)
Frame Rate	100Hz (full format)
Functions	Windowing, Line/row inversion, Image rotation, 2x2 bining

Table 3 : QXGA 7.5µm pitch Read Out Integrated Circuit characteristics.

3.2. PRELIMINARY MEASUREMENTS

Remarkable flip chip with indium bumps has been achieved for this 3 mega-pixels FPA on in-house post-processed ROIC wafers to ensure perfect operability. This is illustrated below by SEM (Scanning Electron Microscopy) image and the following responsivity cartographies obtained on two different QXGA II-VI FPAs with 7.5µm pitch.

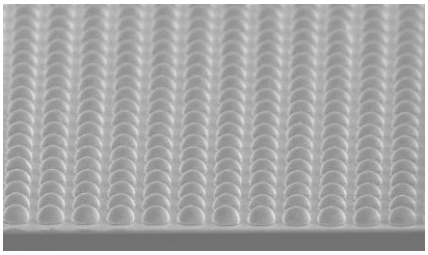

Figure 7 : SEM indium bump image

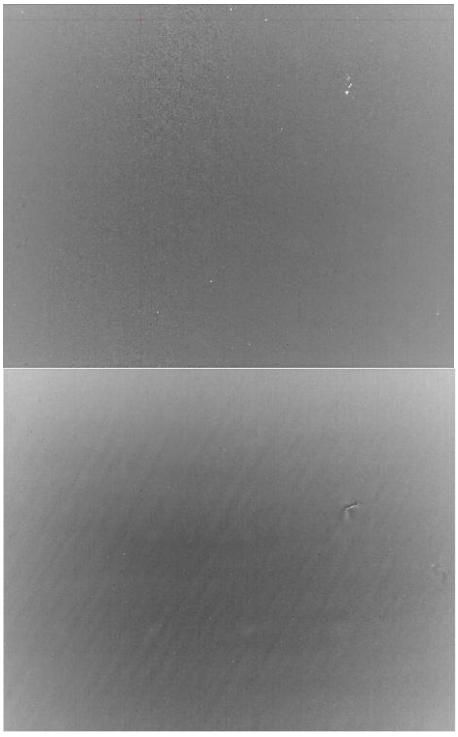

Figure 8 : Responsivity cartographies of two different QXGA FPAs with 7.5µm pitch at 130K

Very uniform responsivity is obtained with a standard deviation below 4% with no indium bumps related macro and micro-defects. Also, a very high level of operability has been achieved for tens of FPA processed, as illustrated below, where 90% of the produced population has an operability above 99.85% with a criteria mean RMS noise ± 100%.

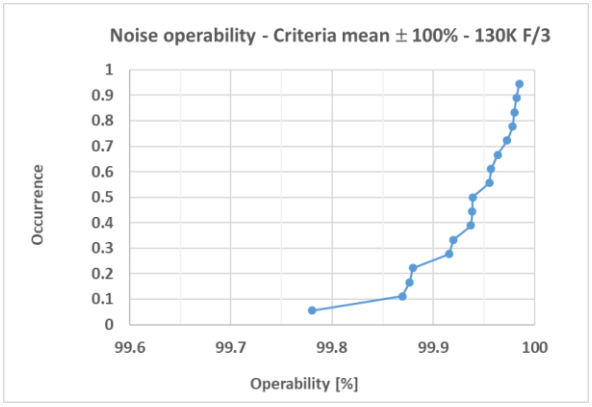

Figure 13 : Noise operability distribution function – 130K F/3 – QXGA 7.5µm pitch

First evaluation of RFPN has been performed, and promising results have been obtained like illustrated below.

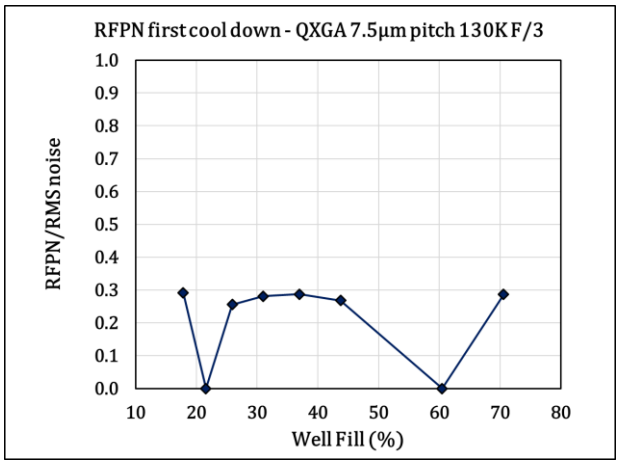

Figure 14 : RFPN to RMS noise ratio at 130K - QXGA products format 7.5µm pitch - F/3 aperture

4. LW PERFORMANCES OPTIMIZATIONS

LWIR detectors for spatial and tactical applications are also continuously being improved. We will detail recent performances improvements in terms of MTF and RFPN.

4.1. MTF IMPROVEMENTS

Following the approach used for the 10µm pitch II-VI technology [10], which consists of maximising the collection volume and minimising the diffusion volume, excellent MTF performance was obtained for the II-VI LW optimized p-on-n technology with 15µm VGA format. An MTF around 0.55 at Nyquist frequency under nominal diode polarisation was recorded.

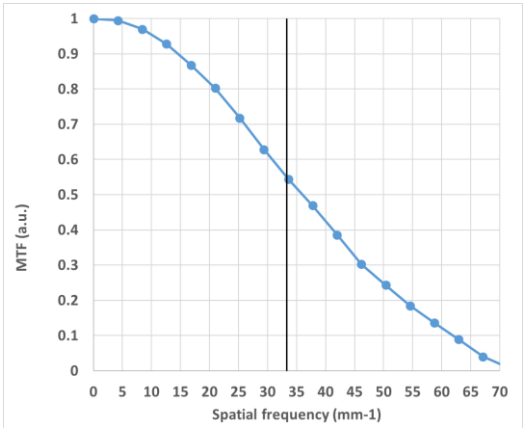

Figure 15 : MTF improvement – 80K – 15µm pitch p-on-n LW technology

This high performance is achieved while maintaining high quantum efficiency around 80% and high minority carrier lifetime with dark current following the Rule 7 law [11]. This represents the theoretical Auger 1 minority carrier recombination limit. The graph below shows the dark current comparison between intrinsic n-on-p technology and extrinsic p-on-n technology, clearly demonstrating a reduction of 2 decades.

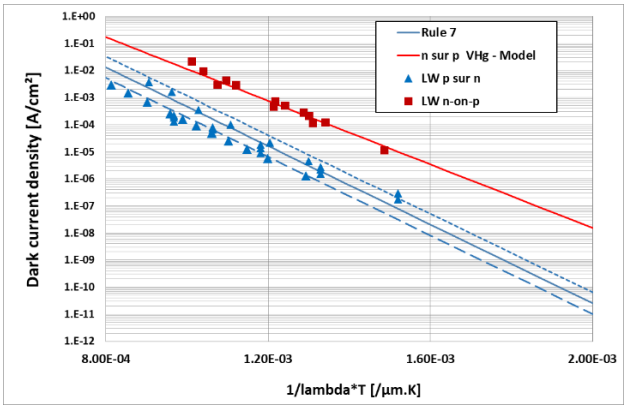

Figure 16 : LW dark current comparison between n-on-p and p-on-n technologies

4.2. RFPN OPTIMZATION

A very low and stable RFPN is obtained. As illustrated below, a RFPN below 0.4 times the temporal noise is obtained for the first cool down. This remains below 0.8 times temporal noise for subsequent cool-downs, with only one point refreshment and in a reproducible way.

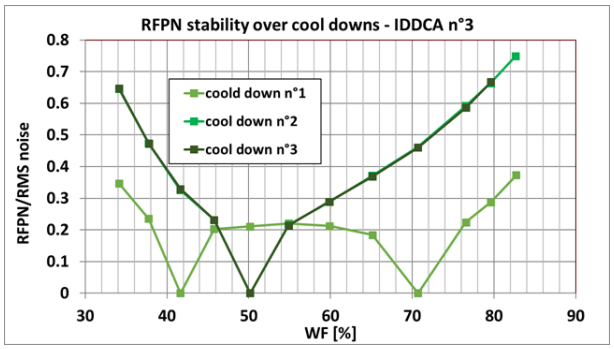

Figure 17 : Stability of RFPN to RMS noise ratio after subsequent cool downs - VGA format 15µm pitch IDDCA – F/2 aperture 80K

This high image quality is achieved throughout the production line. This is demonstrated below for several LW IDDCA with RFPN over temporal noise ratio obtained for the first and second cool downs with only one point refreshment.

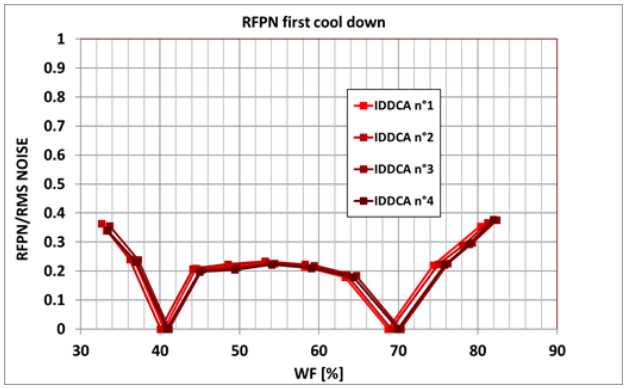

Figure 18 : RFPN to RMS noise ratio for the first cool down - VGA format 15µm pitch IDDCA – F/2 aperture 80K

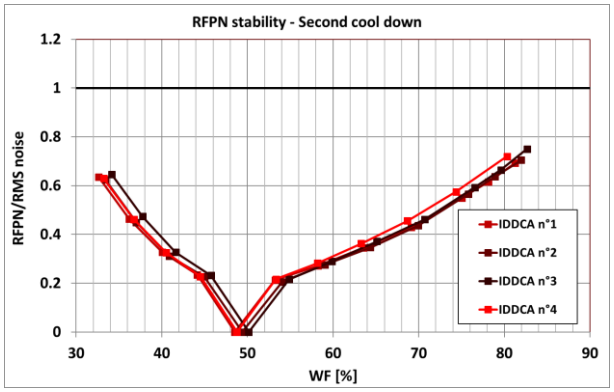

Figure 19 : RFPN to RMS noise ratio for the second cool down - VGA format 15µm pitch IDDCA – F/2 aperture 80K

5. VLW DEVELOPMENT

LYNRED is the European leader in space detectors. Over the past two decades, we have delivered 180 flight models, 80 of which are currently in space for various missions, including defense, scientific research and Earth observation. Following the successful launches of the Meteosat Third Generation missions (one in December 2022 and one in July 2025), we are preparing for the next generation. To this end, we are developing VLWIR detectors with p-on-n technology and a VGA with a 15 µm pitch. We will present the first promising results obtained with this technology.

A 15µm cut-off wavelength at 80 K has been obtained with a quantum efficiency above 80% in the spectral range [7µm, 12µm]. The two graphs below illustrate theses results.

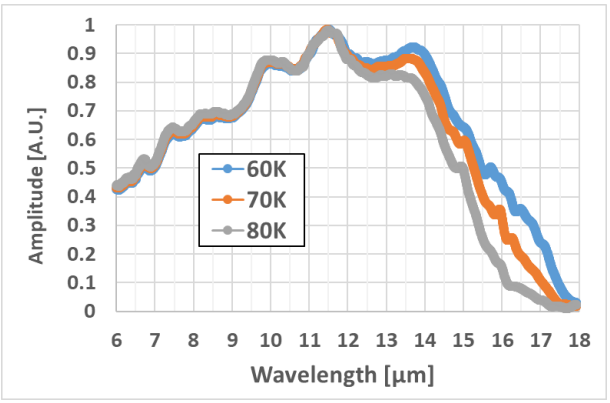

Figure 20 : Normalized spectral response at different temperatures

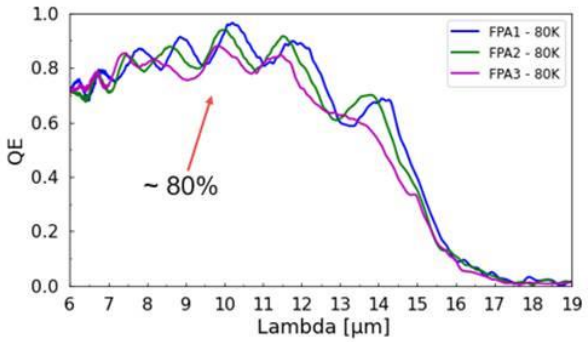

Figure 21 : Quantum efficiency at 80K for three different FPAs

The VLW technology also exhibits a dark current Auger 1 limited. And compared to intrinsic n-on-p technology, we achieved a reduction of at least one decade as shown below.

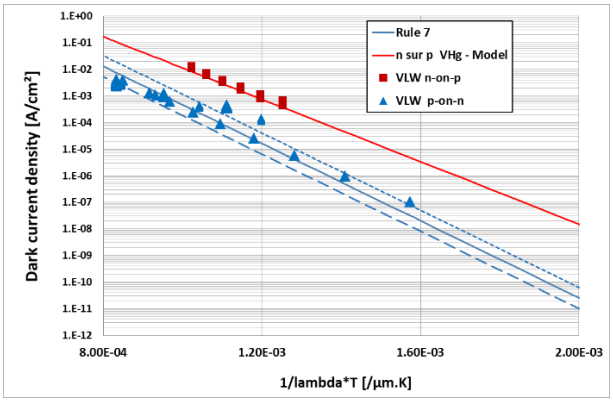

Figure 22 : VLW dark current comparison between n-on-p and p-on-n technologies

This high quantum efficiency and low dark current are completed by an excellent response uniformity, with a standard deviation typically below 3%, as illustrated in the graph below.

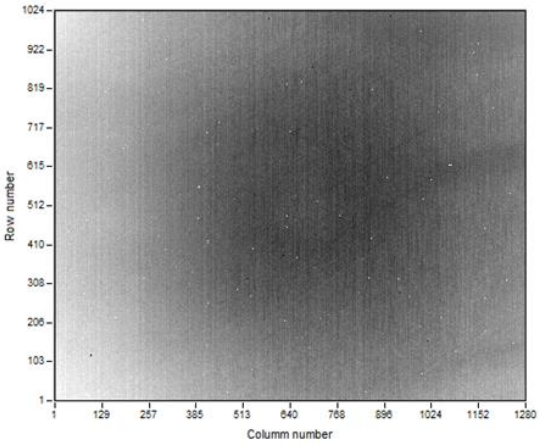

Figure 23 : VLW Responsivity uniformity at 80K- F/2 aperture

Above all, a very high level of operability is achieved. This is demonstrated below with a quasi-perfect Gaussian shape for the temporal noise histogram obtained at 80 K with almost no tail. Operability above 99.8% is then achieved at 80 K with a defect criteria mean noise ± 100%.

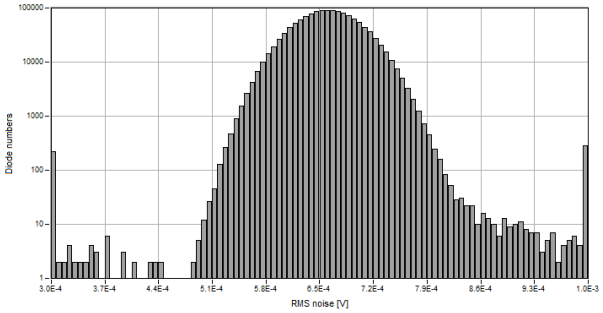

Figure 24 : VLW Temporal noise histogram at 80K – F/2 aperture

6. CONCLUSION

To address the challenge of low SWAPc (Size, Weight and Power cost), LYNRED is developing High Operating Temperature (HOT) II-VI 7.5 µm pitch technology to meet the requirements of applications in the extended MW band. Remarkable performances have been demonstrated at 130K, including EQE close to 85% and MTF of above 0.5 at Nyquist frequency. These achievements are completed by the demonstration of low, stable spatio-temporal noise up to 150 K, indicating the potential for a state-of-the-art QXGA product with a 7.5 µm pitch. This development is particularly promising for high-end and demanding applications requiring the highest achievable range. LYNRED's comprehensive and versatile MW extended band products, which include III-V and II-VI 7.5 µm pitch products with excellent performance and in various formats, ensure they can meet the diverse requirements of customers in the MW extended band. This improvement on HOT mercatel technology has been extended to LW and VLW. For both bands, a very high quantum efficiency of above 80% and a very low dark current, in accordance with the Rule 7 law, have been achieved. The MTF and RFPN have been optimised for LW, and highly promising operability has been achieved at 80 K for VLW with a cut-off wavelength of 15 µm. This makes it highly likely that we will soon achieve the target of increasing the operating temperature by at least 20 K for both bands.

ACKNOWLEDGMENTS

The authors would like to thank all the Lynred and LETI/CEA teams for their dedication to quality work and challenging wins, as well as the French Ministry of Defence for their support of this work.

REFERENCES

[1] O. Gravrand, C. Lobre, J.L. Santailler, N. Baier; W. Rabaud; A. Kerlain, D. Sam-Giao, P. Leboterf, B. Cornus and L. Rubaldo, « Design of a small pitch (7.5µm) MWIR HgCdTe array operating at high temperature (130K) with high imaging performances », Proceedings SPIE 12107, Infrared Technology and Applications XLVIII, 2022.

[2] W.E. Tennant, D. Lee, M. Zandian, E. Piquette, and M.Carmody,"MBE HgCdTe Technology: A very general solution to IR Detection, Described by Rule 07, a very convenient Heuristic," Journal of Electronic Materials, vol. 37, no. 9, pp. 1406–1410, (2014).

[3] I. A. Cunningham et A. Fenster, « A method for modulation transfer function determination from edge profiles with correction for finite-element differentiation », Med. Phys., vol. 14, no 4, p. 533-537, juill. 1987.

[4] J. Berthoz., R. Grille, L. Rubaldo, O. Gravrand, A. Kerlain, N. Pere-laperne, L. Martineau, F. Chabuel, and D. Leclercq « Modeling and characterization of MTF and spectral response at small pitch on Mercury Cadmium Telluride », J. Electron. Mater., vol. 44, no 9, p. 3157-3162, (2015).

[5] S. Machlup, « Noise in semiconductors: spectrum of a two-parameter random signal », J. Appl. Phys. Vol. 25, pp. 341-343, 1954.

[6] D.V. Lang, " Deep-level transient spectroscopy: A new method to characterize traps in semiconductors", J. Appl. Phys. 45, 3023-3032, (1974).

[7] S. Weiss, R. Kassing, "Deep Level Transient Fourier Spectroscopy (DLTFS)-A technique for the analysis of deep level properties", Solid-State Electron.,31, 1733-1742 (1988).

[8] D.L Paula, C.E Jones, "Deep level studies of Hg1−xCdx Te. I: Narrow-band-gap space-charge spectroscopy", J. Appl. Phys., 52, 5118-5131, (1981).

[9] D.L Paula, C.E Jones, " Deep level studies of Hg1−xCdxTe. II: Correlation with photodiode performance", J. Appl. Phys., 52, 5132-5138, (1981).

[10] N. Péré-Laperne, L.Rubaldo, A. Kerlain, E. Carrère, L. Dargent, R. Taalat and J. Berthoz "10µm pitch design of HgCdTe diode array in Sofradir"», *Proc. SPIE Quantum Sensing and Nanophotonic Devices XII*, 9370, 2015..

[11] W.E. Tennant, D. Lee, M. Zandian, E. Piquette, and M.Carmody,"MBE HgCdTe Technology: A very general solution to IR Detection, Described by Rule 07, a very convenient Heuristic," Journal of Electronic Materials, vol. 37, no. 9, pp. 1406–1410, (2014).